ELSEVIER

Journal of Applied Geophysics 51 (2002) 121–129

JOURNAL OF APPLIED GEOPHYSICS

www.elsevier.com/locate/jappgeo

Determining Q of near-surface materials from Rayleigh waves

Jianghai Xia[a,*], Richard D. Miller[a], Choon B. Park[a], Gang Tian[b]

[a] Department of Geology, Kansas Geological Survey, The University of Kansas, 1930 Constant Ave., Campus West, Lawrence, KS 66047-3726, USA

[b] Department of Geophysics, Jinlin University, PR China

Received 19 December 2001; accepted 26 September 2002

Abstract

High-frequency (≥ 2 Hz) Rayleigh wave phase velocities can be inverted to shear (S)-wave velocities for a layered earth model up to 30 m below the ground surface in many settings. Given S-wave velocity (V_S), compressional (P)-wave velocity (V_P), and Rayleigh wave phase velocities, it is feasible to solve for P-wave quality factor Q_P and S-wave quality factor Q_S in a layered earth model by inverting Rayleigh wave attenuation coefficients. Model results demonstrate the plausibility of inverting Q_S from Rayleigh wave attenuation coefficients. Contributions to the Rayleigh wave attenuation coefficients from Q_P cannot be ignored when V_S/V_P reaches 0.45, which is not uncommon in near-surface settings. It is possible to invert Q_P from Rayleigh wave attenuation coefficients in some geological setting, a concept that differs from the common perception that Rayleigh wave attenuation coefficients are always far less sensitive to Q_P than to Q_S. Sixty-channel surface wave data were acquired in an Arizona desert. For a 10-layer model with a thickness of over 20 m, the data were first inverted to obtain S-wave velocities by the multichannel analysis of surface waves (MASW) method and then quality factors were determined by inverting attenuation coefficients.

Keywords: Rayleigh waves; Attenuation coefficients; Quality factors; Near-surface materials

1. Introduction

The most common measure of seismic wave attenuation is the dimensionless quality factor Q and its inverse (dissipation factor) Q^{-1}. The quality factor as a function of depth is of fundamental interest in groundwater, engineering, and environmental studies, as well as in oil exploration and earthquake seismology. A desire to understand the attenuative properties of the earth are based on the observations that seismic wave amplitudes are reduced as waves propagates through an elastic medium. This reduction is generally frequency-dependent and, more importantly, attenuation characteristics can reveal unique information about lithology, physical state, and degree of rock saturation (Toksöz and Johnston, 1981). To fully understand seismic wave propagation in the earth, the quality factors are parameters that must be known. High-frequency Rayleigh waves possesses information of the shear (S)-wave velocity (V_S) and the quality factors of near-surface materials.

* Corresponding author. Tel.: +1-785-864-2057; fax: +1-785-864-5317.

E-mail address: jxia@kgs.ku.edu (J. Xia).

0926-9851/02/$ - see front matter
PII: S0926-9851(02)00228-8

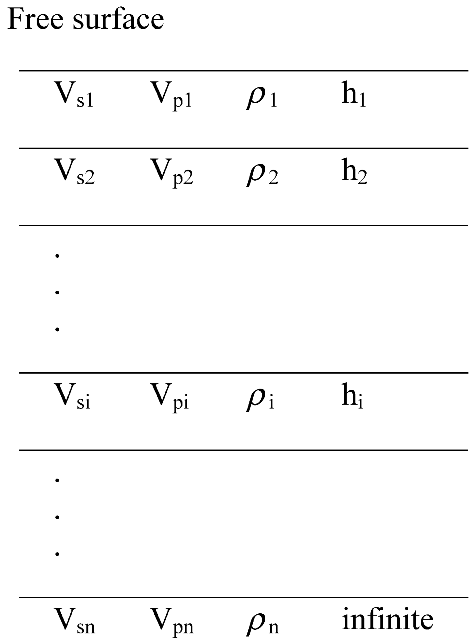

Fig. 1. A layered earth model with parameters of shear-wave velocity (V_S), compressional wave velocity (V_P), density (ρ), and thickness (h).

Rayleigh waves travel along or near the ground surface and are usually characterized by relatively low velocity, low frequency, and high amplitude energy (Sheriff, 1991, p. 143). Estimates of the S-wave velocity from Rayleigh waves and applications to real-world problems have been extensively investigated (Dorman and Ewing, 1962; Aki and Richards, 1980; Stokoe and Nazarian, 1983; Nazarian et al., 1983; Xia et al., 1997, 1998, 1999, 2000a, 2002a,b; Park et al., 1996, 1998, 1999a,b; Miller et al., 1999). Based on the assumption of a layered earth model (Fig. 1), a three-phase research project, multichannel analysis of surface waves (MASW), undertaken by the Kansas Geological Survey (KGS) was designed to estimate near-surface S-wave velocities from high-frequency Rayleigh waves (Fig. 2): (1) acquisition of multichannel high-frequency (≥ 2 Hz) broad band Rayleigh waves; (2) creation of efficient and accurate algorithms organized in a basic data processing sequence designed to extract Rayleigh wave dispersion curves from Rayleigh waves (Park et al., 1999a); and (3) development of stable, robust, and efficient inversion algorithms for inverting phase velocities of Rayleigh waves for near-surface S-wave velocity profiles (Xia et al., 1999).

Based on documented experiences (e.g., Xia et al., 1999, 2000a, 2002b), when the fundamental-mode phase velocities are calculated with a high degree of accuracy, reliable S-wave velocities ($\pm 15\%$) can be estimated. Incorporating higher mode data into the surface wave analysis increases the resolution (or accuracy) of the inverted S-wave velocities (Xia et al., 2000b). After successfully determining a near-

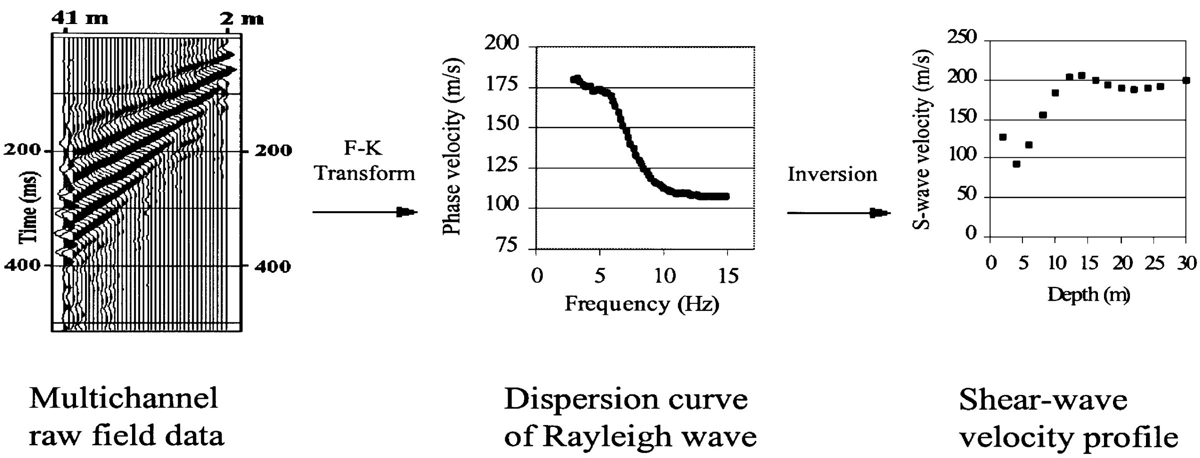

Fig. 2. A diagram of the MASW method. Multichannel raw field data, which contain enhanced Rayleigh wave signals, are acquired. Rayleigh wave phase velocities are extracted from the field data through a direct wavefield transformation method by Park et al. (1998). The phase velocity, finally, is inverted for a shear-wave velocity profile (V_S vs. depth).

surface V_S profile from Rayleigh waves, the feasibility of calculating near-surface Q from high-frequency Rayleigh wave attenuation coefficients can be analyzed.

Laboratory experiments (Johnston et al., 1979) show that Q may be independent of frequency over a broad bandwidth (10^{-2}–10^7 Hz), especially for some dry rocks. Q^{-1} in liquids, however, is proportional to frequency so that in some highly porous and permeable rocks Q^{-1} may contain a frequency-dependent component. This component may be negligible at seismic frequency, even in unconsolidated marine sediments (Johnston et al., 1979). Mitchell (1975) investigated Q structure of the upper crust in the North America by inverting Rayleigh wave attenuation coefficients in a layered earth model. In his work, Q was independent of frequency. Although some authors suggest that near-surface Q may be frequency dependent (Jeng et al., 1999), we will follow the laboratory results (Johnston, 1981) and Mitchell's (1975) work that Q is independent of frequency, allowing determination of Q as a function of depth based on amplitude attenuation of Rayleigh wave data. In this paper, we will examine the relationship between Rayleigh wave attenuation coefficients and compressional P-wave and S-wave quality factors (Q_P and Q_S) through forward modeling. The modeling will be used to develop a quantitative description of the contributions to Rayleigh wave attenuation coefficients from Q_P and Q_S.

2. Basic equations

For a plane wave traveling in a homogeneous medium, the quality factor Q is determined by (Johnston and Toksöz, 1981)

$$Q = \frac{\pi f}{\alpha v}, \tag{1}$$

where v, f, and α are the velocity, the frequency, and the attenuation coefficient of the plane wave, respectively. To determine Q as a function of depth in near-surface materials (up to 30 m), the assumption of homogeneity is no longer valid because of complexity of the near-surface geology. Utilization of high-frequency Rayleigh waves (≥ 2 Hz) is essential in finding the quality factors of near-surface materials. The relationship between Rayleigh wave attenuation coefficients and the quality factors for P- and S-waves of a layered model were given by Anderson et al. (1965) as:

$$\alpha_R(f) = \frac{\pi f}{C_R^2(f)} \times \left[\sum_{i=1}^{n} P_i(f) Q_{Pi}^{-1} + \sum_{i=1}^{n} S_i(f) Q_{Si}^{-1} \right], \tag{2}$$

where

$$P_i(f) = V_{Pi} \frac{\partial C_R(f)}{\partial V_{Pi}}, \tag{3}$$

$$S_i(f) = V_{Si} \frac{\partial C_R(f)}{\partial V_{Si}}, \tag{4}$$

$\alpha_R(f)$ is Rayleigh wave attenuation coefficients in 1/length, and f is frequency in Hz. Q_{Pi} and Q_{Si} are the quality factors for P- and S-waves of the ith layer, respectively; V_{Pi} and V_{Si} are the P-wave velocity and S-wave velocity of the ith layer, respectively; $C_R(f)$ is Rayleigh wave phase velocity; and n is the number of layers of a layered earth model.

We adopted Kudo and Shima's (1970) work to calculate the attenuation coefficients. The attenuation coefficient is defined by

$$A(x + \mathrm{d}x) = A(x) e^{-\alpha \mathrm{d}x}, \tag{5}$$

where A is Rayleigh wave amplitude, α is a Rayleigh wave attenuation coefficient, and x and dx are the nearest source-geophone offset and a geophone interval, respectively. After the Fourier transform with respect to time, we obtain

$$\alpha_R(f) = -\frac{\ln\left[\left| \frac{W(x+\mathrm{d}x, f)}{W(x, f)} \right| \sqrt{\frac{x+\mathrm{d}x}{x}} \right]}{\mathrm{d}x}, \tag{6}$$

where $\alpha_R(f)$ is the Rayleigh wave attenuation coefficient as a function of frequency f, W is the amplitude of a specific frequency, and $\sqrt{\frac{(x+\mathrm{d}x)}{x}}$ is a scaling factor in calculating the attenuation coefficient.

In the following section, contributions of Q_P and Q_S to attenuation coefficients of Rayleigh waves will be analyzed by forward modeling. The sensitivity of Rayleigh wave attenuation coefficients with respect to the dissipation factors, Q_P^{-1} and Q_S^{-1} will also be examined.

3. Modeling results

Eqs. (3) and (4) represent the rate of change of Rayleigh wave attenuation coefficients $\alpha_R(f)$ to dissipation factors Q_P^{-1} and Q_S^{-1} of the ith layer, respectively. P_i is the product of the P-wave velocity of the ith layer and the partial derivative of Rayleigh wave phase velocities with respect to P-wave velocity of the ith layer. S_i is the product of the S-wave velocity of the ith layer and the partial derivative of Rayleigh wave phase velocities with respect to S-wave velocity of the ith layer. P_i and S_i totally control the sensitivity of Rayleigh wave attenuation coefficients to Q_P^{-1} and Q_S^{-1}.

A six-layer model (Xia et al., 1999) is employed to analyze contributions to Rayleigh wave attenuation coefficients from Q_P and Q_S (Fig. 3). Letting V_S change from 25% to 50% of V_P, contributions of Q_P to Rayleigh wave attenuation coefficients increase with increasing V_S/V_P, while Q_S contributions to Rayleigh wave attenuation coefficients decrease as V_S/V_P increases (Fig. 4). Q_P contributions become significant for most frequencies when V_S/V_P approaches 0.45. For example, for the 30 Hz component, when V_S/V_P is 0.5, Q_P contributions dominate and reach more than 70% while Q_S contributions fall to less than 30%. Roughly speaking, when V_S is about one half V_P, overall contributions of Q_P to Rayleigh wave attenuation coefficients may reach more than 30%. This suggests it may be possible to invert Q_P from Rayleigh wave attenuation coefficients when V_S is approximately one half of V_P.

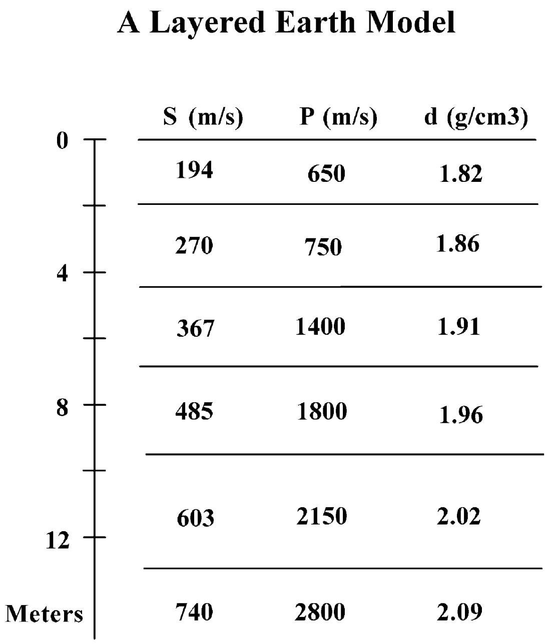

Fig. 3. A layered earth model (Xia et al., 1999) is used to analyze the relationship between attenuation coefficients and quality factors shown in Eq. (2).

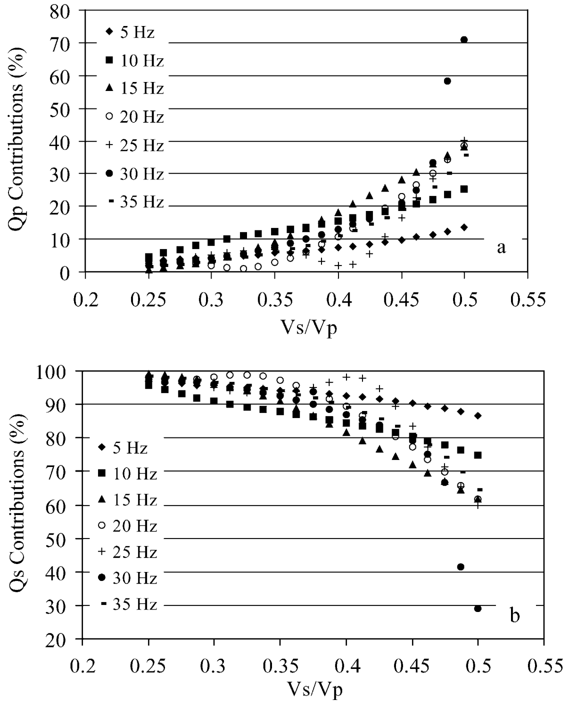

Fig. 4. Q_P contributions to Raleigh wave attenuation coefficients (a) and Q_S contributions to Raleigh wave attenuation coefficients (b). Q_P contributions become significant when V_S/V_P is about 0.5.

Sensitivity of Rayleigh wave attenuation coefficients to Q_P and Q_S is analyzed for the layered model (Fig. 3) when V_S is replaced by 50% of V_P. For a dry sandstone, Q_P/Q_S is almost equal to one (Johnston, 1981), making Q_P and Q_S equal (5, 10, 12, 15, 20, and 25 from the top layer to the half space). A 25% reduction in Q_P and/or Q_S (3.75, 7.5, 9.0, 11.25,

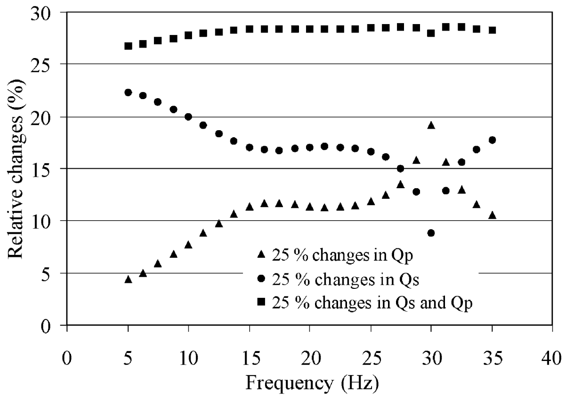

Fig. 5. Sensitivity of Rayleigh wave attenuation coefficients to Q_P and Q_S with V_S/V_P being equal to 0.5.

15.0, and 18.75 from the top layer to the half space) results in the relationship shown in Fig. 5. With a 25% reduction in Q_P, the relative increases in Rayleigh wave attenuation coefficients are in the range of 4–20%, averaging 12% from 5 to 35 Hz. For the same reductions in Q_S, the relative increases in Rayleigh wave attenuation coefficients are in the range of 9–23% with an average of 17% from 5 to 35 Hz. The overall relative increases in Rayleigh wave attenuation coefficients due to a 25% reduction in both Q_P and Q_S are almost the same at 28% in relative change within the frequency range of 5–35 Hz. For a water saturated sandstone, Q_P/Q_S may reach 2 (Johnston, 1981). In that case, the contributions to Rayleigh wave attenuation coefficients due to Q_P may surpass those due to Q_S.

4. Inversion system

Eq. (2) manifests the linear relationship between Rayleigh wave attenuation coefficients and the dissipation factors for P- and S-waves (Q_P^{-1} and Q_S^{-1}). Theoretically, after determining S-wave velocities by inverting Rayleigh wave phase velocities (Xia et al., 1999) and finding near-surface P-wave velocities by other seismic methods, such as reflection (Hunter et al., 1984; Steeples and Miller, 1990), refraction (Palmer, 1980), and/or tomography methods (Zhang and Toksöz, 1998; Ivanov et al., 2000), the dissipation factors (Q_P^{-1} and Q_S^{-1}) can be inverted directly for noise-free data using Eq. (2). Practically, however, our modeling results indicate that surface wave attenuation is sensitive enough to Q_P when V_S/V_P is over 0.45. Otherwise, surface wave attenuation is far less sensitive to Q_P than to Q_S, and only Q_S can be inverted from Rayleigh wave attenuation coefficients.

Because Eq. (2) is a linear system, the same method used in Xia et al. (1999) can be employed directly to solve Q_P and/or Q_S from Rayleigh wave attenuation coefficients. In many cases, only a single iteration is necessary to obtain quality factors. Here we discuss an algorithm from Menke (1984) including our introduction of a damping factor. Our inversion problem can be described by the following system:

$$\mathbf{A}\vec{X} = \vec{B}\,(x_i > 0), \tag{7}$$

where $\vec{X}$ is an inverse of quality factors (a model vector $1/Q$) with x_i as the ith component, $\vec{B}$ is attenuation coefficients (a data vector), and $\mathbf{A}$ is a data kernel matrix (Menke, 1984) determined by Eq. (2).

Eq. (7) will provide accurate Q_P and Q_S if attenuation coefficients contain no error as a synthetic example shows in the following section. Solutions of Eq. (7) are not guaranteed to exist or solutions may possess an unacceptable error when attenuation coefficients possess errors. Mitchell (1973, 1975) discussed the method of solving the inverse problem presented in Eq. (7). A damping factor λ is introduced.

$$(\mathbf{A} + \lambda\mathbf{I})\,\vec{X} = \vec{B}\,(x_i > 0), \tag{8}$$

where $\mathbf{I}$ is the unit matrix. λ is set to be a small value (say 10^{-7}) at the beginning of the inversion. Based on inverted results of Q_P and/or Q_S, λ will be systematically increased until smooth solutions are obtained.

5. A synthetic example

The purpose of this example is to show the inversion system (Eq. 8) working properly. With a six-layer model, this example assumes known P-wave and S-wave velocities (Fig. 6a), error-free attenuation coefficients (labeled "Measured" in Fig. 6b), Q_S (5, 10, 12, 15, 20, and 25 for layer one to the half space, respectively), and Q_P (twice of Q_S). Attenuation coefficients (labeled "Measured" in Fig. 6b) were inverted to quality factors. Fig. 6c shows inverted Q_P

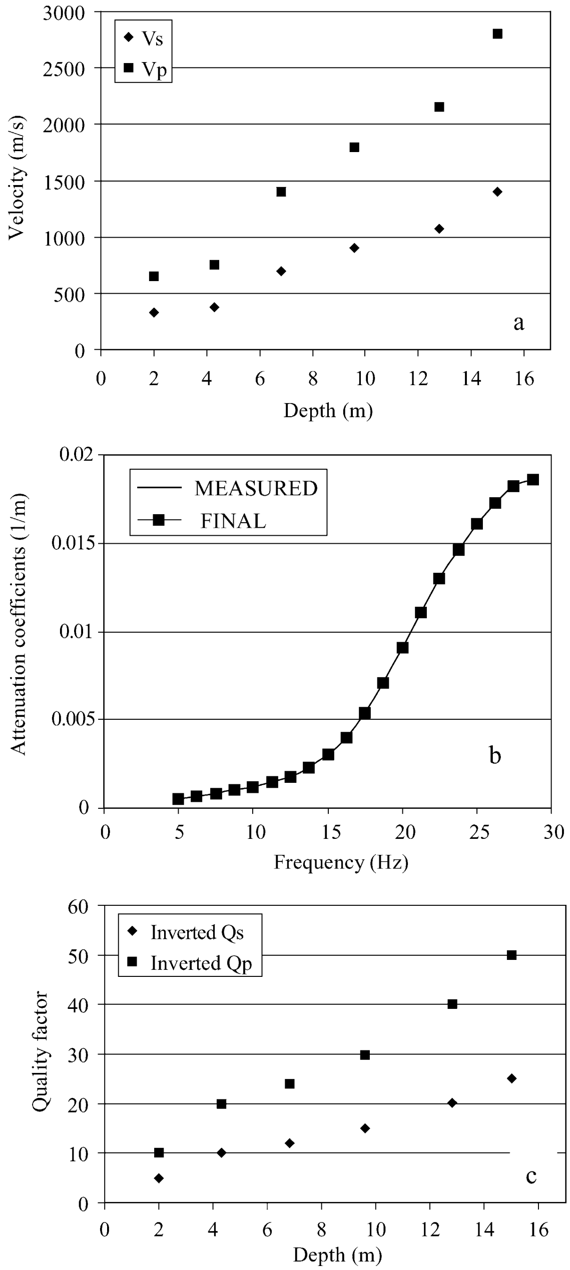

Fig. 6. A synthetic example. (a) P-wave and S-wave velocities of a six-layer model. (b) Input data: assumed known attenuation coefficients labeled "Measured" and calculated attenuation coefficients labeled "Final" based on inverted quality factors in (c).

and Q_S that are exactly equal to values of the known model and attenuation coefficients calculated from inverted Q_P and Q_S (labeled "Final" in Fig. 6b).

6. A real-world example

Sixty-channel surface wave data were acquired using 4.5 Hz vertical geophones in an Arizona desert (Fig. 7). Geophones were deployed at 1.2-m intervals with a nearest offset of 4.8 m. The seismic source was an accelerated weight drop designed and built by the KGS. A record length of 1024 ms at a 1-ms sample interval was selected.

The number of layers of a model should be determined by the quality of data (Xia et al., 2000b). A layer in a model is usually not a geological layer. In most case, we choose 10 to 15 layers in a model to obtain certain resolution for an inverted model. For this particular data, a 10-layer model with a total thickness of 20 m was used to invert Rayleigh wave phase velocities to S-wave velocities (Fig. 8a) by the MASW method (Xia et al., 1999; Park et al., 1999a).

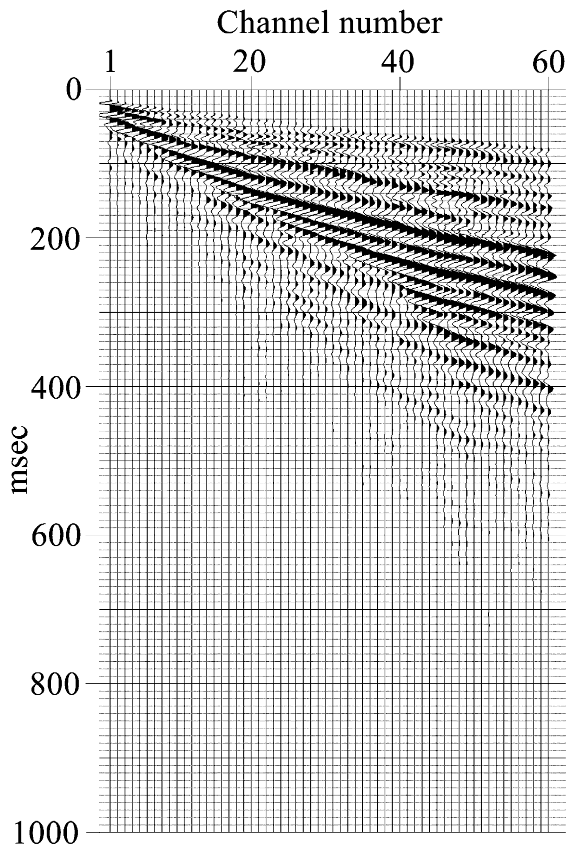

Fig. 7. Sixty-channel raw field data acquired in an Arizona desert. See the text for details.

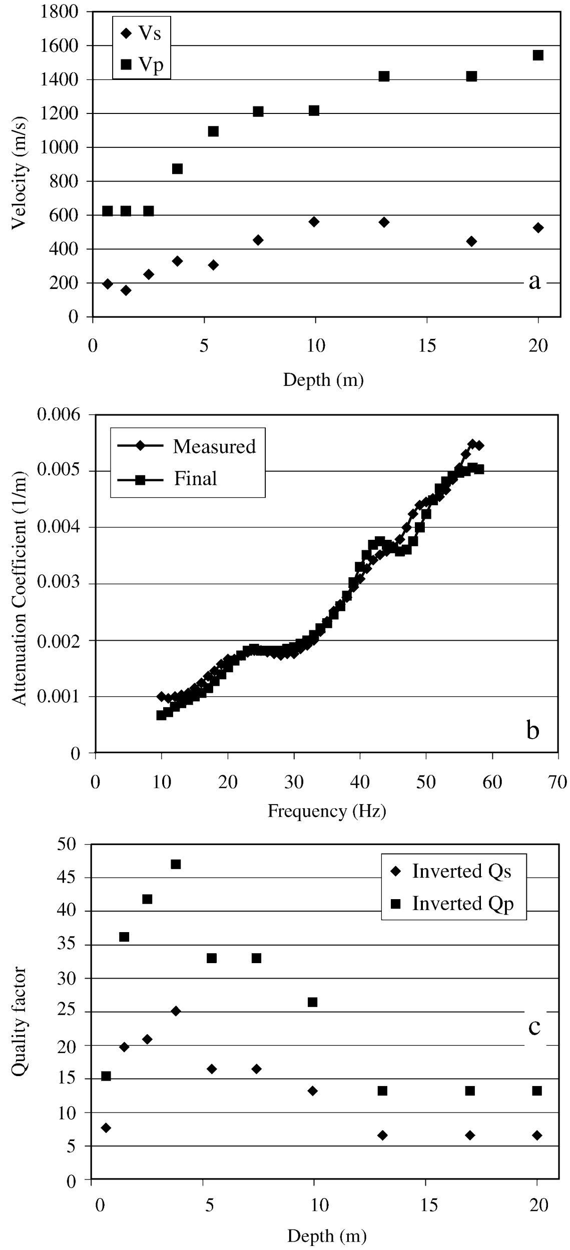

Fig. 8. Inversion results from data in Fig. 7. (a) Inverted S-wave velocities of a 10-layer model by using the MASW method with P-wave velocities determined based on the first arrivals of the input data. (b) Attenuation coefficients labeled "Measured" were calculated by Eq. (6) and those labeled "Final" were calculated based on the inverted quality factor model (c).

P-wave velocities of the model were determined by the first arrivals of the data (Fig. 7). Attenuation coefficients of Rayleigh waves (labeled "Measured" in Fig. 8b) were calculated by using Eq. (6). Because an average ratio of V_S/V_P for the model is approximately 0.4, only Q_S can be confidently inverted from attenuation coefficients. Under the assumption that Q_P was equal to twice Q_S, we inverted attenuation coefficients to obtain Q_S (Fig. 8c). Attenuation coefficients calculated from inverted quality factors Q_S were labeled "Final" in Fig. 8b. Inverted Q_S results suggested that there is a highly attenuating layer at a depth of 12.5 m.

7. Discussion and conclusions

Modeling results and the real-world example demonstrated a feasibility of inversion of attenuation coefficients of Rayleigh waves for quality factors. Modeling analysis also showed that Q_P may be inverted when V_S/V_P is greater than 0.45, a situation which is common in oil industry and crust seismology studies, and which is not also uncommon in near-surface materials. Modeling results also suggested that most contributions to Rayleigh wave attenuation coefficients from Q_P are in a relatively higher frequency range, while contributions from Q_S are in a lower frequency range. Using different weighting, therefore, on Q_P and Q_S in different frequency ranges may increase the possibility of obtaining Q_P.

In the synthetic and real examples, we assumed $Q_P = 2Q_S$ to obtain information of Q_P. Inverted results will be changed if a different relationship between Q_P and Q_S is assumed. The relationship between Q_P and Q_S could vary in a wide range for near-surface materials so it may be necessary to use some other methods to find Q_P or provide a crosscheck.

Based on the sensitivity analysis, errors in inverted quality factors can reach 1 to 1.5 times the error in attenuation coefficients. Compared to the inversion system that Xia et al. (1999) developed to invert S-wave velocities from Rayleigh wave phase velocities (10% error in surface wave phase velocity will result in 6% error in S-wave velocity), Eq. (8) has less stability. Hence, accurate calculation of Rayleigh wave attenuation coefficients is critical. On the other hand, the inversion system (Eq. (8)) is more stable than AVO (amplitude versus offset) analysis studied and practiced in the oil industry for the last 20 years (Hilterman, 2001). Jin et al. (2000) concluded that in AVO analysis, a 10% error in incident angles could result in a 40% error in reflection coefficients. Because our geophysical community accepts AVO practices, we should be more comfortable with quality factors that are inverted from Rayleigh wave attenuation coefficients.

Acknowledgements

We thank Prof. J.A. Canas and one anonymous reviewer for their critical and constructive reviews, which improved the paper. The authors thank Mary Brohammer and Julia Shuklaper for their assistance in manuscript preparation and submission.

References

Aki, K., Richards, P.G., 1980. Quantitative Seismology—Theory and Methods. Freeman, San Francisco.

Anderson, D.L., Ben-Menahem, A., Archambeau, C.B., 1965. Attenuation of seismic energy in upper mantle. J. Geophys. Res. 70, 1441–1448.

Dorman, J., Ewing, M., 1962. Numerical inversion of seismic surface wave dispersion data and crust-mantle structure in the New York–Pennsylvania area. J. Geophys. Res. 67, 5227–5241.

Hilterman, F.J., 2001. Seismic amplitude interpretation. Distinguished Short Course 4. Society of Exploration Geophysicists and European Association of Geoscientists and Engineers.

Hunter, J.A., Pullan, S.E., Burns, R.A., Gagne, R.M., Good, R.L., 1984. Shallow seismic reflection mapping of the overburden-bedrock interface with the engineering seismograph—some simple techniques. Geophysics 49, 1381–1385.

Ivanov, J., Park, C.B., Miller, R.D., Xia, J., Hunter, J., Good, R.L., Burns, R.A., 2000. Joint analysis of surface-wave and refraction events from river-bottom sediments. Technical Program with Biographies, Society of Exploration Geophysicists, 70th Annual Meeting, Calgary, Canada. Society of Exploration Geophysicists, Tulsa, OK, pp. 1307–1310.

Jeng, Y., Tsai, J., Chen, S., 1999. An improved method of determining near-surface Q. Geophysics 64, 1608–1617.

Jin, S., Cambois, G., Vuilermoz, C., 2000. Shear-wave velocity and density estimation from PS-wave AVO analysis: application to an OBS dataset from the North Sea. Geophysics 65, 1446–1454.

Johnston, D.H., 1981. Attenuation: a state-of-the-art summary. In: Toksöz, M.N., Johnston, D.H. (Eds.), Seismic Wave Attenuation. Society of Exploration Geophysicists, Tulsa, OK, pp. 123–135.

Johnston, D.H., Toksöz, M.N., 1981. Definitions and terminology. In: Toksöz, M.N., Johnston, D.H. (Eds.), Seismic Wave Attenuation. Society of Exploration Geophysicists, Tulsa, OK, pp. 1–5.

Johnston, D.H., Toksöz, M.N., Timur, A., 1979. Attenuation of seismic waves in dry and saturated rocks: II. Mechanisms. Geophysics 44, 691–711.

Kudo, K., Shima, E., 1970. Attenuation of shear wave in soil. Bull. Earthq. Res. Inst. 48, 145–158.

Menke, W., 1984. Geophysical Data Analysis—Discrete inversion Theory. Academic Press, New York.

Miller, R.D., Xia, J., Park, C.B., Ivanov, J., 1999. Multichannel analysis of surface waves to map bedrock. Lead. Edge 18, 1392–1396.

Mitchell, B.J., 1973. Surface wave attenuation and crustal anelasticity in central North America. Bull. Seismol. Soc. Am. 63, 1057–1071.

Mitchell, B.J., 1975. Regional Rayleigh wave attenuation in North America. J. Geophys. Res. 80, 4904–4916.

Nazarian, S., Stokoe II, K.H., Hudson, W.R., 1983. Use of spectral analysis of surface waves method for determination of moduli and thicknesses of pavement systems. Transp. Res. Rec. 930, 38–45.

Palmer, D., 1980. The Generalized Reciprocal Method of Seismic Refraction Interpretation. Society of Exploration Geophysicists, Tulsa, OK.

Park, C.B., Miller, R.D., Xia, J., 1996. Multi-channel analysis of surface waves using Vibroseis (MASWV). Expanded Abstracts of Technical Program with Biographies, Society of Exploration Geophysicists, 66th Annual Meeting, Denver, CO. Society of Exploration Geophysicists, Tulsa, OK, pp. 68–71.

Park, C.B., Miller, R.D., Xia, J., 1998. Imaging dispersion curves of surface waves on multi-channel record. Technical Program with Biographies, Society of Exploration Geophysicists, 68th Annual Meeting, New Orleans, LA. Society of Exploration Geophysicists, Tulsa, OK, pp. 1377–1380.

Park, C.B., Miller, R.D., Xia, J., 1999a. Multichannel analysis of surface waves. Geophysics 64, 800–808.

Park, C.B., Miller, R.D., Xia, J., Hunter, J.A., Harris, J.B., 1999b. Higher mode observation by the MASW method. Technical Program with Biographies, Society of Exploration Geophysicists, 69th Annual Meeting, Houston, TX. Society of Exploration Geophysicists, Tulsa, OK, pp. 524–527.

Sheriff, R.E., 1991. Encyclopedic Dictionary of Exploration Geophysics, 3rd ed. Society of Exploration Geophysicists, Tulsa, OK.

Steeples, D.W., Miller, R.D., 1990. Seismic-reflection methods applied to engineering, environmental, and ground-water problems. In: Ward, S.H. (Ed.), Geotechnical and Environmental Geophysics 1. Society of Exploration Geophysicists, Tulsa, OK, pp. 1–30.

Stokoe II, K.H., Nazarian, S., 1983. Effectiveness of ground improvement from spectral analysis of surface waves. Proceeding of the Eighth European Conference on Soil Mechanics and Foundation Engineering, Helsinki, Finland. A.A. Balkema Publishers, Netherlands, pp. 91–95.

Toksöz, M.N., Johnston, D.H., 1981. Preface. In: Toksöz, M.N., Johnston, D.H. (Eds.), Seismic Wave Attenuation. Society of Exploration Geophysicists, Tulsa, OK, pp. v–vi.

Xia, J., Miller, R.D., Park, C.B., 1997. Estimation of shear wave velocity in a compressible Gibson half-space by inverting Rayleigh wave phase velocity. Expanded Abstracts of Technical Program with Biographies, Society of Exploration Geophysicists, 67th Annual Meeting, Dallas, TX. Society of Exploration Geophysicists, Tulsa, OK, pp. 1927–1930.

Xia, J., Miller, R.D., Park, C.B., 1998. Construction of vertical section of near-surface shear-wave velocity from ground roll. Technical Program, The Society of Exploration Geophysicists and The Chinese Petroleum Society, Beijing 98' International Conference. Chinese Petroleum Society, Beijing, pp. 29–33.

Xia, J., Miller, R.D., Park, C.B., 1999. Estimation of near-surface shear-wave velocity by inversion of Rayleigh wave. Geophysics 64, 691–700.

Xia, J., Miller, R.D., Park, C.B., Hunter, J.A., Harris, J.B., 2000a. Comparing shear-wave velocity profiles from MASW with borehole measurements in unconsolidated sediments, Fraser River Delta, B.C., Canada. J. Environ. Eng. Geophys. 5 (3), 1–13.

Xia, J., Miller, R.D., Park, C.B., 2000b. Advantage of calculating shear-wave velocity from surface waves with higher modes. Technical Program with Biographies, Society of Exploration Geophysicists, 70th Annual Meeting, Calgary, Canada. Society of Exploration Geophysicists, Tulsa, OK, pp. 1295–1298.

Xia, J., Miller, R.D., Park, C.B., Hunter, J.A., Harris, J.B., Ivannov, J., 2002a. Comparing shear-wave velocity profiles from multichannel analysis of surface wave with borehole measurements. Soil Dyn. Earthqu. Eng. 22 (3), 181–190.

Xia, J., Miller, R.D., Park, C.B., Wightman, E., Nigbor, R., 2002b. A pitfall in shallow shear-wave refraction surveying. J. Appl. Geophys. 51 (1), 1–9.

Zhang, J., Toksöz, M.N., 1998. Nonlinear refraction traveltime tomography. Geophysics 63, 1726–1737.